Establishing the Credibility of Computational Models of Blood Pumps

Through Verification, Validation, and Uncertainty Quantification

AUTHORS
MARK S. GOODIN AND M. ERTAN TASKIN

Originally published as Chapter 18 in
Computational Modeling and Simulation of Medical Devices: Verification, Validation, and Uncertainty Quantification

About This Technical Chapter

Computational modeling and simulation can provide valuable insight into the performance, safety, and reliability of blood-contacting medical devices. For blood pumps in particular, however, the usefulness of a model depends not only on the quality of the simulation, but also on the credibility of the methods, assumptions, validation practices, and supporting evidence behind it.

In this published chapter, SimuTech Group engineers Mark S. Goodin and M. Ertan Taskin explore how verification, validation, and uncertainty quantification can be applied to computational models of blood pumps. Their discussion includes the use of risk-informed credibility frameworks, the relationship between simulation and physical testing, and practical considerations for evaluating model reliability in medical-device development.

The chapter also examines how credible computational modeling can support engineering decisions involving blood-flow performance, device design, potential blood damage, testing strategies, and regulatory review.

Originally published as Chapter 18 in *Computational Modeling and Simulation of Medical Devices: Verification, Validation, and Uncertainty Quantification*, this work reflects SimuTech Group's commitment to advancing reliable, evidence-based simulation practices for the medical-device industry.

The complete chapter is reproduced in the following pages in its original published form. SimuTech Group has added this introductory page, the cover, and the closing material. No changes have been made to the original chapter content.

Original Publication

Chapter: "Establishing the Credibility of Computational Models of Blood Pumps Through Verification, Validation, and Uncertainty Quantification"
Authors: Mark S. Goodin and M. Ertan Taskin
Published in: *Computational Modeling and Simulation of Medical Devices: Verification, Validation, and Uncertainty Quantification*
Publisher: Springer Nature

Chapter 18
Establishing the Credibility of Computational Models of Blood Pumps Through Verification, Validation, and Uncertainty Quantification

Mark S. Goodin and M. Ertan Taskin

1 Introduction

Cardiovascular diseases are the leading cause of death globally, causing about 32% of all deaths worldwide, with 85% of those due to heart attack and stroke [1]. Mechanical circulatory support (MCS) has become the standard of care for patients with advanced heart failure refractory to maximal medical therapy [2]. Medical therapies may vary depending on the level of the disease, patient condition, and donor availability factors. For example, patients may need to be (a) temporarily supported during a procedure or part of a procedure (short-term support), (b) supported until transplantation (bridge to transplant), or (c) supported during their lifetime (destination therapy). Considering the criticality of the need, a tremendous amount of time and effort has been spent to develop devices capable of supporting heart failure patients.

This chapter focuses on blood pumps that are designed to satisfy the aforementioned use cases. It begins by providing a history of extracorporeal support. Key performance parameters for blood pumps, including those specific to the longer use and higher risk ventricular assist devices (VADs), are then introduced and discussed. An overview of the computational modeling methods typically used for simulating circulatory support devices is then provided. Building upon this foundation, the next sections review two case studies that utilize the ASME V&V40 risk-based framework to establish the credibility of models used to assess VAD performance on the bench and in patients. The chapter concludes by providing examples of potential questions of interest for blood pumps and considering future modeling developments that could further advance the role of computational modeling and simulation for circulatory support devices. A table summarizing different blood pump-related performance

M. S. Goodin (✉) · M. Ertan Taskin
SimuTech Group, Rochester, NY, USA
e-mail: mgoodin@simutechgroup.com

M. Horner et al. (eds.), *Computational Modeling and Simulation of Medical Devices*,
https://doi.org/10.1007/978-3-032-09180-2_18

parameters, their clinical significance, and associated validation methods is also provided. References for the articles describing the computational fluid dynamics (CFD) modeling and supporting validation work are also included in this summary table.

2 Brief History of Mechanical Circulatory Support

The beginning of the enhancements in the field of MCS dates back to the middle of the nineteenth century with the first patented roller pump in 1855 by Porter and Bradley. Truax then patented the first double-roller pump for transporting blood in 1899, as shown in Fig. 1 [3]. The first major improvement for MCS was achieved in 1934 with the modifications by DeBakey, whose pump was used in one of the first heart–lung machines [3]. Since then, many extracorporeal and implanted ventricular assist devices (VADs) have been introduced.

As in the case of the initial roller pump concept, extracorporeal support devices are mainly used to provide blood perfusion for oxygenation in patients with cardiac or pulmonary failure. In 1968, a centrifugal "low-hemolysis" device was developed, known as the "BioPump," which was commercialized in 1976 [4]. In the early 2000s, a similar centrifugal device, called the CentriMag was developed for extracorporeal membrane oxygenation (ECMO) [5].

VADs are mechanical pumps that are implanted to help the heart pump blood throughout the body. In general, VADs can be classified into two distinct categories: pulsatile and continuous flow. The former, also known as the first-generation

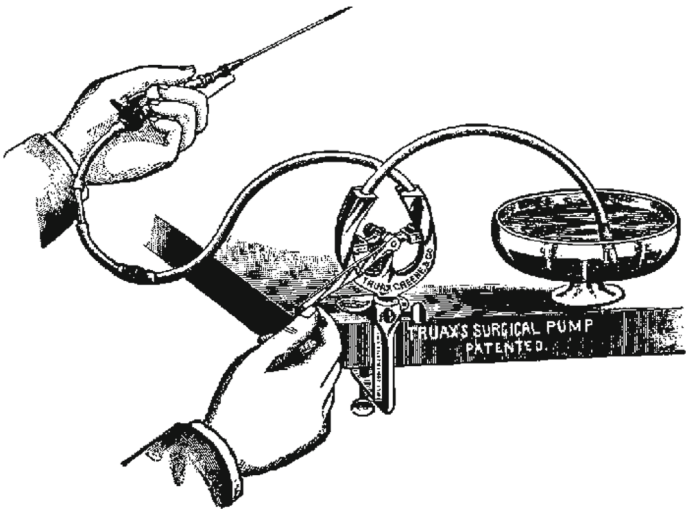

Fig. 1 Truax roller pump

blood pumps, are based on the volume displacement concept. The currently unavailable Abbott HeartMate I (HMI) was an implantable example of this class. Another example is the pulsatile Berlin Heart Excor blood pumps, which are extracorporeal devices that still support pediatric and adult patients worldwide. Continuous flow devices typically use a rotary pumping concept that can be axial, centrifugal, or mixed flow. The early application of an axial bloop pump was introduced by Wampler et al. in 1988 [6]. Also known as the "Hemopump," this device was intended to provide support to the left ventricle, with access through the femoral artery. Leveraging turbine technology developed by NASA engineers, a group of doctors led by DeBakey developed a small axial flow blood pump [7]. Following these enhancements, Jarvik introduced a similar axial flow pump known as the Jarvik 2000 [8]. And one of the most popular implanted axial blood pump applications was the Abbott HeartMate II (HMII). The Jarvik 2000 and Heartmate II pumps use contact bearings and/or seals, and therefore, they would be considered second-generation blood pumps [4].

The most recent VADs incorporate contactless bearings for maintaining the rotor-to-stator clearance. Considered third-generation designs, the two prominent bearing technologies used in left ventricular assist devices (LVADs) are: (1) hydrodynamic bearing and passive magnetic rotor levitation (used in the Medtronic HVAD pump [9]) and (2) fully magnetic rotor levitation (used on the Abbott HM3 pump [10]). Although the HVAD pump is no longer currently on the market, it provided life support for more than 20,000 patients [11]. Today, the HM3 pump is providing life support to patients with reduced adverse events. Even though both devices are considered continuous flow pumps, they use different types of speed modulation algorithms to produce a pulsatile operation. The blood flow path through the Medtronic HVAD is shown in Fig. 2.

Key milestones in the development of MCS are summarized in Table 1 [12], which starts from the initial VAD implantation in the early 1960s and ends with the first demonstration of the superiority of LVAD therapy in 2001. It is also important to note that there are many pumps and technologies mentioned in this section that led to breakthroughs in the industry and facilitated different designs and technologies that are in use today [13].

3 Classifications and Design Features of Blood Pumps

(a) **Continuous and Pulsatile Flow Pumps**: As described in Sect. 2, blood pumps are typically classified as pulsatile or continuous flow. Historically, more continuous flow pumps have been developed than pulsatile flow pumps. Mimicking the native pulsation of the heart and fully perfusing the vascular bed is a potential inadequacy of continuous flow pumps that is still under debate [14]. Furthermore, the current complications associated with LVADs are related to the non-pulsatile nature of these devices, such as gastrointestinal bleeding, arteriovenous malformations, hemolysis, pump thrombosis, and aortic insufficiency

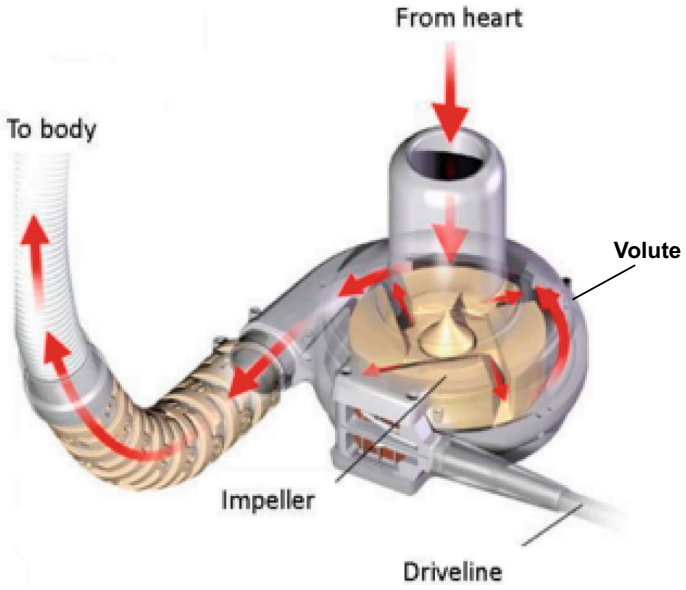

Fig. 2 Blood flow paths through Medtronic HVAD pump [9]

Table 1 Early milestones in the development of mechanical circulatory support

Year	Milestone
1963	First VAD implantation
1964	NHLBI founds the Artificial Heart Program
1969	First TAH implantation
1972	NHLBI initiates an LVAD program
1975	NHLBI sponsors clinical trials of pneumatic LVADs
1980	Request for proposals for untethered electric, portable LVADs
1991	First implantation of electric, portable LVAD
1994	First patient discharges from hospital with portable LVAD
2001	REMATCH trial demonstrates superiority of LVAD over optimal medical therapy in New York Heart Association Class IV patients

[15]. Nevertheless, given the reliability and relative simplicity of continuous flow blood pumps, the pulsatile volume displacement pumps have nearly disappeared [14]. To address the potential complications associated with a lack of pulsatility, newer continuous blood pump designs are capable of either optional or compulsory speed modulation functions to introduce pulsatile flow operation. A positive clinical impact was demonstrated in terms of reduced stroke rates when the speed cycle pulsation option was utilized [16]. Numerical analysis has indicated that pump wash out could be increased with compulsory speed

modulation, which aligns with clinically reported lower thrombotic complications [17]. Note that improvements in pump wash out may correlate with more streamlined flow throughout the pump and therefore may be associated with decreased pump thrombosis [18].

(b) **Peristaltic (Roller) Pumps**: As already mentioned, the earliest continuous flow blood pump applications were roller pumps. The concept is to move the blood in an enclosed tubing where the tube is squeezed while it is mechanically deformed by a roller. Currently, peristaltic pumps are primarily used for extracorporeal support during cardiopulmonary bypass procedures, which last up to several hours. Their main advantages are reliability, due to their simplicity, and lower cost. However, blood damage and tubing spallation are key disadvantages of this design [13].

(c) **Rotary Blood Pumps (RBPs)**: As part of the continuous flow family, energy is transferred to the fluid by velocity changes within the impeller vanes of a RBP. Therefore, based on the geometric features of the impeller and the housing, RBPs can be classified as axial, radial (or centrifugal), and mixed flow pumps. The pump is classified as axial when the pump inflow and outflow are on the same axis and as centrifugal when the pump outflow is perpendicular to the inflow. The pump is classified as mixed flow when the inflow and outflow points are located in between [14]. The size, and consequently the required speed, are determined based on the pump classification. For example, axial pumps can be smaller in size compared to centrifugal pumps, and thus, the impeller rotational speed required to generate a similar output would be greater. RBPs have outstanding potential, given their physiological and technological advantages such as implantability, transportability, and lower anticoagulation levels. However, RBPs can carry increased hemolytic and thrombotic risks due to induced high mechanical shear stress [13].

(d) **Blood Pumps with Bearings**: Rotary blood pumps may use different bearing mechanisms to maintain the position of the impeller. For example, mechanical pivot bearings provide physical contact between the impeller and the housing. One weakness is that wear may lead to local frictional heating and/or local blood flow wash out issues [19]. Nonetheless, there are many long-term support VADs available in the industry using this technology. Contactless bearings are also widely used in VADs with the intent of longer-term use. Among them, hydrodynamic bearings are purely passive, where the bearing gap depends on the bearing load (which is mostly defined by the rotational speed) and is usually in the range of micrometers. This technology relies on increased pressure between the hydrodynamic bearing and the housing surfaces which then creates a load. Hydrodynamic bearings could be used for either radial or axial rotor support, depending on the type of pump [20]. Precise machining is required since this technology uses relatively small gaps. Similarly, the small gaps may lead to high fluid shear stress, thus initiating hemolysis [21]. Finally, active magnetic bearings are more sophisticated because of the required control mechanisms for stable impeller operation. While these bearings do not require small gaps, the overall size of the device can increase since the bearing forces are proportional

to the magnet volume. Also unlike hydrodynamic bearings, magnetic levitation (maglev) technology allows for suspension of the impeller in multiple directions (both radial and axial), with the ability to control the bearing clearance.

4 Blood Pump Performance Parameters

Blood pump performance is evaluated based on a variety of factors, ranging from assessing the hydrodynamic environment (e.g., flow patterns and shear stress) to ensuring sufficient longevity inside the patient (e.g., susceptibility to hemolysis and thrombosis). This section reviews some of the more critical concerns in pump design.

(a) **Hydrodynamics**

A VAD's hydraulic performance is determined by its ability to provide patients with the required blood flow rate over a wide range of conditions. A sufficient blood flow rate is needed during periods of low activity, such as while resting or sleeping, as well as more active situations including walking or climbing stairs. Hydraulic performance is characterized by the relationship between the generated pressure head (H) and the flow rate (Q). Hydraulic performance is typically characterized using H-Q curves (see Fig. 3) and varies by pump type [14]. For example, axial flow pump H-Q curves are typically steeper than centrifugal pump curves and have a higher shut-off pressure (low or no flow condition). Therefore, the centrifugal pumps can produce higher pressures at high flow rates, whereas the axial pumps generate higher pressure at low flow rates.

VADs are typically designed to have their optimum hydraulic performance at an operating condition that is most often experienced by the patient, such as a blood flow rate of 4 L/min and a pressure rise of 100 mmHg. However, the VAD must also function acceptably over a range of blood flow rates, e.g., from 1 to 7 L/min, and pump pressure levels, e.g., from 30 to 150 mmHg. The pump's ability to quickly respond to changing patient hemodynamics is also an important factor.

(b) **Pump Efficiency**

Pump efficiency is another parameter used to define blood pump performance. Overall pump efficiency combines hydraulic, mechanical, and electronic aspects to convey how well the pump is designed over a wide range of operating conditions. Figure 4 shows a typical pump efficiency chart for different impeller rotational (operating) speeds. Note how the peak in the efficiency curves slightly shifts for different operating speeds. Since the pump is designed to reach a pressure head at a specified rotor speed, the highest efficiency is achieved at the corresponding operating "design point" for that specified rotor speed. Also note that the maximum efficiency levels of blood pumps can be less than that for industrial pumps, which can achieve pump efficiencies greater than 70% [22]. This is because the pump efficiency is not the ultimate performance parameter for blood pumps. Designers must also consider biocompatibility, which is at least as important as the pump's efficiency, and may lead to a compromise on the design to achieve lower hemolysis or thrombus potential.

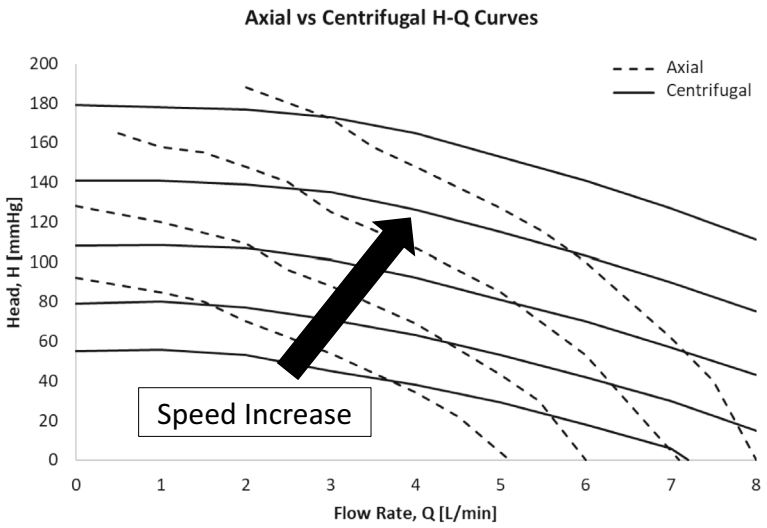

Fig. 3 Typical axial and centrifugal pump H-Q curves. Different curves are for different rotor speeds of corresponding pump types

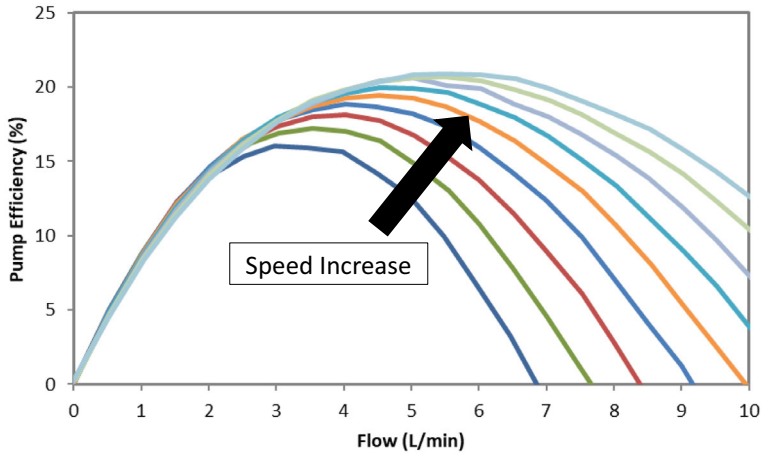

Fig. 4 Typical overall pump efficiency chart for blood pumps. Different color curves represent different impeller rotational (operating) speeds

(c) **Biocompatibility**

The overall, long-term biocompatibility of VADs is reported using Kaplan–Meier survival curves. Figure 5 shows the percentage survival of different types of LVADs and therapies versus years after transplant [23]. Note that Kaplan–Meier survival curves for blood pumps account for complications due to many reasons, including

both patient-specific and clinical conditions. Adverse events also impact survival rates. These could be procedure related, such as neurologic events, thrombus ingestion from the atrium or ventricle, air embolization, and coagulopathic bleeding. Other adverse events could occur post-implantation, such as device or components malfunction, thromboembolism, hemolysis, and infection [24].

VADs are designed with relatively thromboresistant materials and employ effective washing of the pump surfaces to reduce the risk of thrombus formation and thromboembolic events [24]. However, these biocompatibility-related effects are still observed during the therapy, typically resulting from reduced local washing and low or high shear regions. Formation and growth of thrombus within the device can alter the pump hemodynamics and performance, causing increased power consumption and reduced cardiac output. Thrombus formation and thromboembolism are extremely complicated phenomena, but can be monitored by measuring platelet activation.

Another design concern is hemolysis, which occurs when elevated shear forces rupture erythrocytes (red blood cells), causing the hemoglobin within the erythrocytes to leak into the surrounding plasma. A patient with functioning kidneys can remove damaged red blood cells, and therefore, blood pumps are designed to meet clinically acceptable hemolysis rates. However, clinically significant hemolysis could still be observed in such cases as kinking or blockage of inflow/outflow conduits or acute valvular insufficiency [24]. Hemolysis is typically monitored with lactate dehydrogenase counts clinically and with plasma-free hemoglobin concentration measurements during in vitro experiments. Representative platelet activation and hemolysis curves are shown in Fig. 6 [25].

(d) **Durability**

VADs are intended to provide life support for a time duration that is based on the therapy. For example, it could be months to years for bridge to transplant or bridge

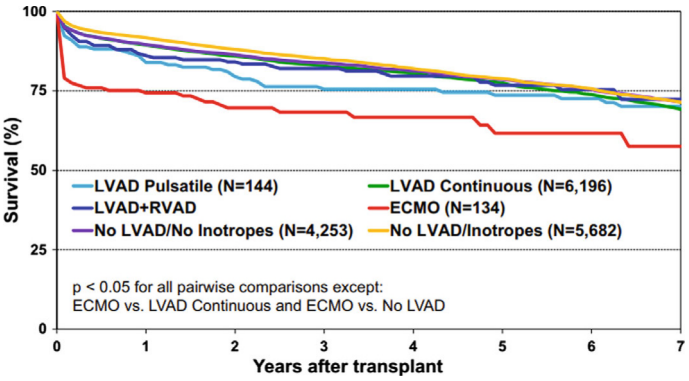

Fig. 5 Kaplan–Meier survival by pre-transplant mechanical circulatory support use (adult heart transplants: January 2009 to June 2016). ECMO, extracorporeal membrane oxygenation; LVAD, left ventricular assist device; RVAD, right ventricular assist device [23]

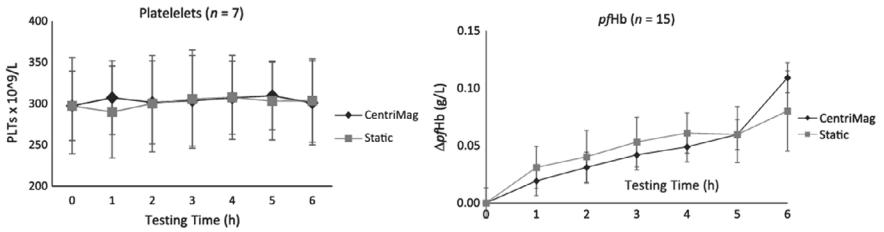

Fig. 6 Representative platelet activation (left) and hemolysis (right) curves [25]

to recovery therapies, respectively. It could also be multiple years to decades for destination therapies. Therefore, each and every VAD component has to be designed to provide crucial life support and enhance the quality of the life for heart disease patients while minimizing the potential for adverse events. For example, endurance testing of VADs is conducted to demonstrate the functionality of the pump beyond its expected length of use. Such testing evaluates the reliability of both the pump components and the software used to control the pump's operation.

(e) **Anatomical Considerations**

As previously described, VAD size depends on pump classification, e.g., whether it is an axial or radial flow design. Important anatomical considerations include sizing a pump to fit inside the pericardial sac to eliminate the need for a pump pocket and having a flat bottom surface that fits on the diaphragmatic surface of the heart [26]. The size and shape of current third-generation continuous flow devices can accommodate these different anatomical aspects.

5 CFD Modeling of Blood Pumps

The primary goals of modeling blood pumps are to predict pump hydraulic performance, efficiency, and biocompatibility. These performance parameters depend on a CFD model that accurately captures the flow patterns within the pump. Shear stress experienced by the flowing blood is one CFD-predicted quantity of particular importance. The shear stress on the impeller surfaces is used to determine the rotor torque, which is multiplied by the impeller rotational speed to calculate the power requirements and efficiency of the pump. Also, shear stress and the local exposure time of the blood are typically used to predict blood damage quantities such as platelet activation, thrombus formation, and hemolysis. In this section, we will provide an overview of the key CFD modeling steps and parameters used to achieve these goals when modeling VADs.

An accurate geometrical representation of the pump's internal flow path that captures the small, and often significant, design features is the starting point for blood pump CFD modeling. Such important features typically include the inflow and outflow regions, the curvature of the impeller blades, the clearance between the

impeller blades and the pump housing, the bearing region, and if applicable, the volute design. The next step is to create a computational mesh that preserves these features and resolves the velocity field near the VAD's internal surfaces. Mesh sensitivity studies assess the change in predicted local quantities, such as shear stress and exposure time, and global quantities, such as average pressure rise and impeller torque, with increasing levels of mesh refinement [27]. Numerous CFD software packages have been used to solve the Navier–Stokes equations for modeling blood pumps [28–30]. The key decisions related to setting up the pump simulations include: (a) specifying the blood material properties, (b) selecting an appropriate turbulence model, (c) using a steady-state or transient flow approach, and (d) choosing a method for assessing pump biocompatibility.

(a) **Blood Material Properties**

Blood is typically modeled using a constant density value that is slightly greater than water, and either a constant (Newtonian) or shear-rate dependent (non-Newtonian) viscosity. Blood is a shear-thinning fluid, where the viscosity increases at shear strain rates below 100–200/sec [26, 31]. However, most of the flow volume in a VAD will experience shear strain rates above this threshold and so blood will behave as a nearly constant viscosity fluid [29] (note that reported value for the constant viscosity varies somewhat in the literature, see, for example, [31, 32]). However, lower shear strain rates may occur in separated or recirculating flow regions, with a corresponding increase in the local viscosity. In such cases, using a non-Newtonian blood viscosity model could improve CFD model predictions related to thrombus formation, which is more likely to occur in lower shear, longer residence time regions.

(b) **Turbulence Modeling**

Given the fluid properties of blood, along with the dimensions and impeller rotational speeds of VADs, low Reynolds number turbulent flow conditions will predominate throughout the pump. Two-equation Reynolds Averaged Navier–Stokes (RANS) models are typically used to account for turbulent flow effects. These two-equation models solve for the turbulent kinetic energy (k) and either the turbulent dissipation rate (ε) or the turbulent specific dissipation rate (ω). The hybrid model proposed by Menter improves accuracy in both near-wall boundary layers and free-stream regions by blending the k-ω model in the near-wall region with the k-ε model away from the wall. For example, this approach is better able to predict the onset of flow separation compared with standard k-ε or k-ω models alone [33]. More complex turbulence models account for directional variations in the turbulent flow and resolve the larger turbulent eddies away from the walls, rather than use empirical relationships [34, 35]. It is also important to note that laminar flow conditions may exist within narrow flow paths of a pump, such as in the bearing regions. Therefore, it is important that the selected turbulence model can return laminar flow results in the near-wall region. Alternatively, some CFD solvers allow for the designation of flow regions as being explicitly laminar or turbulent. This capability could be used a priori to define these narrow flow regions as laminar when creating the simulation.

(c) **Steady-State or Transient Flow**

CFD solvers typically include a multiple reference frame methodology that is able to model rotating bodies embedded in stationary regions. This is implemented by creating a cylindrical volumetric region surrounding the rotating impeller that defines the rotating frame of reference. The remaining pump volume is modeled in the stationary reference frame. An interface is then created in the CFD code that connects the rotating and stationary flow regions. Two types of steady-state simulations are typically used for modeling pumps: "Frozen Rotor" and "Staged." The "Frozen Rotor" method fixes the impeller at one rotational position and transfers the local velocities and pressures across the interface. This method is commonly used for blood pumps where it's important to fully capture the impeller flow field exiting into the volute or cylindrical-shaped housing regions. The "Staged" method also uses a fixed impeller rotational position but averages the momentum and pressures when transferring the flow field results across the interface. Multi-stage rotary machines, where one-time mixing losses occur at each subsequent rotor-to-stator interface, often use this method. Lastly, a full transient simulation rotates the impeller in time, capturing a time-accurate flow field at each time step. The transient effects on the flow field as the impeller spins, such as identifying areas of sustained low or high shear stress, can be captured with this approach. A "Frozen Rotor" solution is often used as an initial condition for transient simulations. Multiple revolutions of the impeller are typically modeled to achieve time-periodic CFD results, thus minimizing the impact of initial conditions on the flow solution [26].

(a) **Assessing Pump Biocompatibility**

Being able to qualitatively, if not yet quantitatively, gain insight into the likelihood (and regional distributions) of blood damage is of tremendous value to those developing new blood pumps. Therefore, a significant amount of work has been reported and is still ongoing related to the use of computational modeling to predict pump-related blood damage, including hemolysis, platelet activation, and thrombosis. For hemolysis, early efforts focused on using empirical relationships based on shear stress and exposure time to predict cell lysis. For example, the following equations rely on empirical constants (A, β, and, α) obtained by regressing experimental data, where a range of values for these parameters have been reported [36–39].

$$\text{Hemolysis Index(HI)} = \text{Damage Index(D)} = \Delta\text{Hgb/Hgb},$$
$$\text{Hemolysis Index(HI)} = \text{Damage Index(D)} = A * \tau^{\beta} * t^{\alpha},$$

where:

Hgb	hemoglobin concentration (g/dl)
A	constant
τ	local shear stress (Pa)
β	shear exponent
t	exposure time (sec)
α	time exponent

Note that ΔHgb represents the change in hemoglobin concentration after one pass through a pump. Levels of shear stress that could cause instantaneous hemolysis, as well as the application of Lagrangian and Eulerian methods to calculate cumulative and regional hemolysis generation rates, have been explored [40–44]. Typically, calibration of the constants used in the empirical relationship is required to align the CFD-predicted results with the in vitro measured values.

More recent efforts have focused on predicting levels of platelet activation and thrombus formation [45]. The platelet activation methods parallel those used for predicting hemolysis and are based upon shear stress and exposure time [46]. Methods that predict thrombus formation include reactions that mimic the clotting cascade, platelet adhesion on internal surfaces, as well as changes to the flow path due to thrombus growth and thrombus ingestion [47, 48].

6 Brief Overview of the ASME V&V40 Standard

The ASME V&V40 [49] standard presents a risk-based framework that can be used to demonstrate the credibility of a computational model when answering a question of interest for a given context of use. The framework outlines a series of steps that help identify the credibility requirements of a computational model. First, the question of interest "describes the specific question, decision, or concern that is being addressed." [49] Next, the context of use (COU) "describes the role and scope of the computational model used to inform that decision in relation to other evidence." Model risk is based upon the combination of model influence and decision consequence when answering the question of interest for the defined COU. Model influence is the relative contribution of the computational model relative to other available information, and decision consequence is the potential severity of an adverse outcome from making an incorrect decision. Adverse outcomes include potential harm to the patient as well as clinical and financial negative outcomes. Model credibility is demonstrated using a series of credibility factors that assess the rigor needed in the V&V process for the specific application. The reader is referred to Chap. 5 or the standard itself for more comprehensive information.

7 Case Studies Applying the ASME V&V40 Framework to Ventricular Assist Devices

There are currently a limited number of case studies available in which the ASME V&V40 framework has been applied to VAD design and evaluation. Among them, one work is related to the FDA blood pump round-robin study where different risk assessments were demonstrated for two different contexts of use [50]. In the other study, a VVUQ plan was implemented for a left ventricle device (LVAD) system

[51]. These case studies are briefly summarized in this section with a focus on how the ASME V&V 40 standard can be used to help establish that the computational model has sufficient credibility.

(a) **Case Study 1: Assessing Computational Model Credibility Using a Risk-Based Framework: Application to Hemolysis in Centrifugal Blood Pumps** [50].

This article demonstrated the application of the ASME V&V40 framework for a centrifugal blood pump. Two hypothetical scenarios were explored: (1) The pump is used to support a patient undergoing cardiopulmonary bypass, and (2) the pump provides short-term ventricular assistance. For this discussion, we will focus on the implanted VAD application, using the centrifugal pump design from the FDA round-robin blood pump study shown in Fig. 7a [50, 52]. This VAD is intended to operate from 2 to 6 L/min at impeller rotational speeds between 2500 and 3500 revolutions/min (rpm). Figure 7b shows contours of wall shear stress on the surfaces of the pump at the highest blood flow rate and impeller rotational speed condition of 6 L/min at 3500 rpm [50].

A description of the different meshing methods, CFD software, turbulence models, and input parameters used to model this centrifugal pump is provided in the FDA round-robin study summary article [52]. A constant blood density and viscosity matching the in vitro test conditions was used for these simulations. In addition, an Eulerian power-law hemolysis model was used to predict the hemolysis level at each flow condition. Measured static pressures at the pump's inlet and outlet, particle image velocimetry (PIV), and in vitro hemolysis testing were used to validate the CFD-predicted pump pressure rise, velocity field, and the flow-related hemolysis

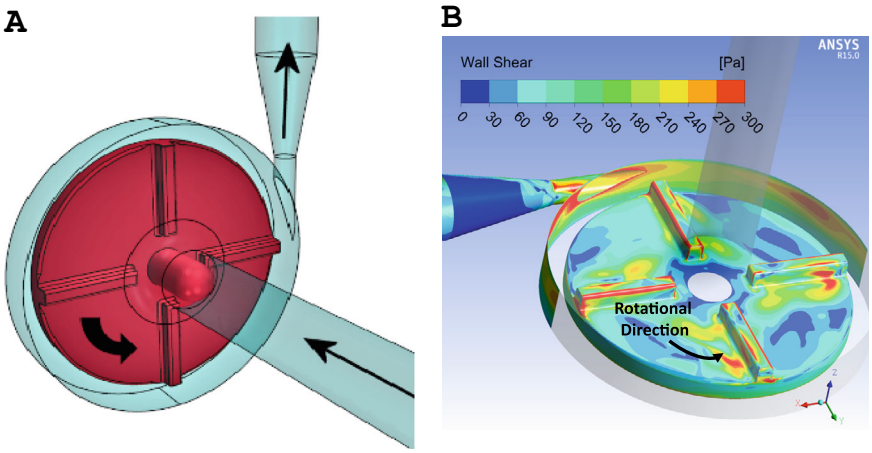

Fig. 7 **a** Geometry and flow direction for the centrifugal blood pump used in the FDA round-robin study. **b** CFD results showing contours of wall shear stress at 6 L/min and 3500 rpm, with the upper range limited to 300 Pa to assist in identifying higher shear stress regions [50, 52]

[52, 53]. The overall goal of the study was to determine if the CFD model provides sufficient credibility in predicting hemolysis over the VADs full operating range.

For this example, the **question of interest** was "are the flow-induced hemolysis levels of the centrifugal pump acceptable for the intended use?"

The **COU** for the VAD application (article COU #2) was built upon the knowledge gained through the cardiopulmonary bypass application (article COU #1). This knowledge included using the CFD model to predict the two potentially worst-case flow/speed conditions for hemolysis. PIV and in vitro hemolysis testing were performed at those conditions, and at one additional low flow condition, to validate the CFD model flow field and hemolysis predictions. For the VAD application, the scope was expanded to use the CFD model in predicting the flow field and hemolysis at two additional extreme operating conditions where in vitro data was not available.

The **quantities of interest (QoIs)** were the pump's hydraulic performance, velocity flow field, blood shear stress, blood exposure time, and flow-induced hemolysis level. The CFD model incorporated an Eulerian power-law hemolysis model to compare with the in vitro hemolysis measurements.

Model Risk Assessment

The **model influence** was categorized as HIGH as the evaluation of pump safety and effectiveness was based solely upon the CFD results at two of the pump's extreme operating conditions.

The **decision consequence** was also categorized as HIGH because surgical intervention and/or device replacement may be required should this implanted pump cause increased hemolysis. Either of these scenarios puts the patient at a significantly increased risk.

Considering the HIGH levels for model influence and decision consequence, the model risk map in Table 2 assigns a model risk of HIGH.

Model Credibility

Verification: For this HIGH-risk application, the code and calculation verification sections of the article: (1) discussed the verification of the Eulerian power-law model using benchmarks from a previously published study, (2) described the grid convergence approach, (3) quantified the discretization error for both velocity and hemolysis (the primary quantity of interest), and (4) provided software quality assurance documentation. The article also reviewed the challenges in verifying the turbulence and Eulerian-based hemolysis models.

Table 2 FDA blood pump VAD application—risk map

Decision Consequence	Low	Med	High
High	3	4	5 ★
Med	2	3	4
Low	1	2	**3**

Model Influence

Validation: The model validation study consisted of particle image velocimetry (PIV) measurements with a blood-analog fluid and hemolysis measurements using porcine or human blood [52, 53]. The PIV experiments provided both hydraulic performance data and velocity profile measurements at multiple locations within the pump. The hemolysis testing was conducted using both the FDA blood pump and a clinically approved VAD for direct comparison of the hemolysis results. An acceptable hemolysis threshold for the FDA blood pump was based upon the hemolysis levels encountered in a commercially available VAD. All hemolysis results were reported as relative values that were normalized to this threshold. The PIV and hemolysis evaluations were both repeated five times for each operating condition. The experimental fluctuations and uncertainty in the model inputs, including the fluid properties, flow rate, and impeller rotational speed, were then quantified. The uncertainty in the model outputs (flow velocity and hemolysis level), due to the uncertainty in the model inputs, was calculated using a Monte Carlo-based method to meet the desired level of rigor for the output comparison.

Applicability: The primary quantity of interest, the hemolysis level, is identical for the computational model and the comparator. Concerning relevance of the validation activities to the COU, the three validation points spanned the operating conditions with increased potential for generating hemolysis, thereby achieving the desired level of credibility.

Summary: Given the uncertainty for both the CFD-predicted and experimentally measured relative hemolysis values, this study found acceptable levels of hemolysis at validation condition 1, as shown in Fig. 8. At the second and third validation conditions, the uncertainty in both the test data and CFD model results suggests that hemolysis levels may exceed the relative hemolysis threshold value of 1. Assuming a mean comparison error and experimental uncertainty that is similar to condition 1, the authors conclude that the pump will not cause unacceptable levels of hemolysis at condition 4. For the other untested condition 5, however, the model form and other sources of uncertainties would not provide sufficient credibility for predicting acceptable levels of hemolysis. This means that the CFD-predicted hemolysis levels are not sufficiently credible across the entire pump operating range. Therefore, additional evidence is required to understand whether the hemolysis levels caused by the pump are acceptable. This might include animal testing and/or comparing measured hemolysis levels for the new blood pump with those for a currently marketed, predicate blood pump.

(b) **Case Study 2: Design and Execution of a Verification, Validation, and Uncertainty Quantification Plan for a Numerical Model of Left Ventricular Flow After LVAD Implantation.**

This example focuses on the impact of the flow distortions introduced by LVAD implantation in the left ventricle, which may lead to thrombus [51]. The study framework combines experimental and numerical aspects in a highly detailed manner as shown in Fig. 9 [51]. For example, certain variables such as heart rate, ejection fraction, and systemic parameters were extracted from benchtop experiments to specify

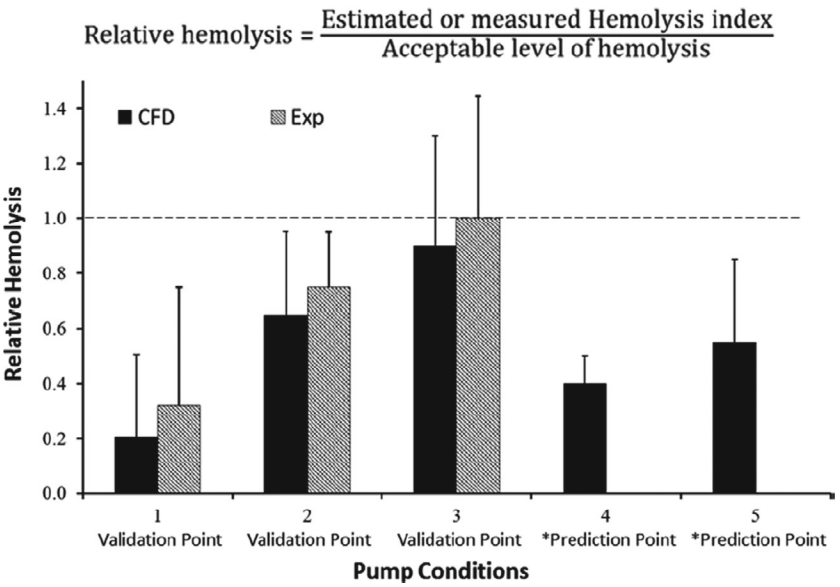

Fig. 8 Hemolysis results at three validation conditions and two prediction-only conditions, as indicated by an asterisk. The CFD results are normalized to the hemolysis observed in the predicate device; therefore, a Relative Hemolysis of 1 would represent clinically acceptable hemolysis levels. Note that the results reported in this article for the experimental and CFD-predicted hemolysis are hypothetical

simulation boundary conditions that can be used as part of uncertainty quantification. The simulations use a deformable ventricle model with unidirectional fluid–structure interaction (FSI). A pressure-driven valve model mimics mitral and aortic valve operation. The model does not include the pump geometry; instead, the pump function was prescribed using H-Q curves at an inflow cannula geometry attached to the apex of the ventricle.

The **question of interest** was "for an apically implanted LVAD, does the selected pump speed: (a) achieve complete aortic valve opening and (b) provide sufficient cardiac output for a range of HR and EF expected for a heart failure patient population?" The assumption was that flow stagnation was associated with insufficient or low flow. Therefore, sufficient cardiac output and aortic valve opening would facilitate better ventricular washing and lower stagnation potential.

The **COU** was described as creating a heart-LVAD computational model that can assist design engineers in preclinical development of the LVAD by characterizing the aortic root, LVAD, and intra-left ventricle flows as a function of pump speed. The goal was to create a computational model capable of replicating their benchtop experiments for quantitative analyses as part of parametric explorations that span the expected range of HR and EF for heart failure patients. The benchtop experiments were performed using a mock circulation loop of the heart and circulatory system, including an apically implanted LVAD.

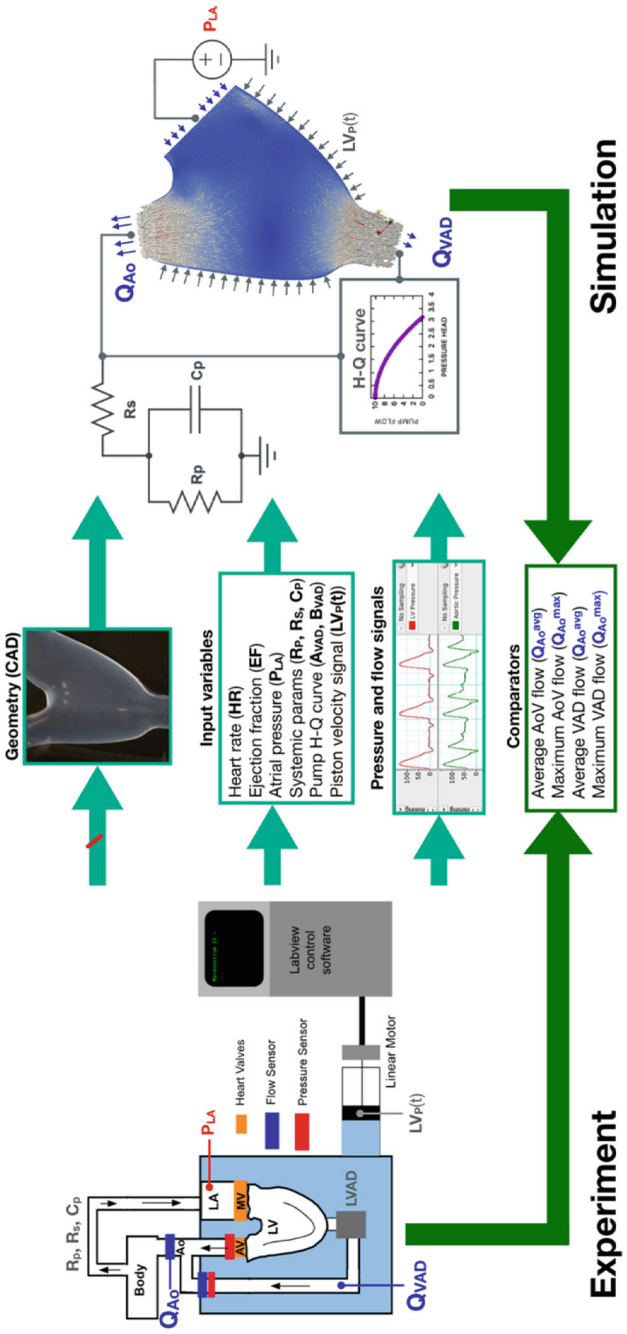

Fig. 9 Overview of the experimental and numerical framework used in the LVAD study [51]

The **QoIs** were the simulation outputs relevant to the COU and question of interest, which are the flow rates through the aortic root and LVAD.

Model Risk Assessment

The **model influence** was categorized as LOW since further animal testing and clinical trials are expected to follow the numerical studies.

The **decision consequence** was categorized as HIGH. While the COU specifies the model will be used for design iteration, the results could be used to make indirect decisions that affect the patients' health. For example, a model that fails to make accurate predictions for the question of interest could suggest an operating condition that produces either: (a) low cardiac output or (b) a permanently closed aortic valve. These might lead to thromboembolic events, aortic regurgitation, or even death.

Considering the model influence and decision consequence, the model risk map in Table 3 assigns a model risk level of MEDIUM.

Model Credibility:

Verification: The verification activities were executed based on flow conditions similar to the ones typically found in the left ventricle. Numerical code verification was executed for a 2D Poiseuille and 3D Womersley flow problem in a cylindrical tube, considering the analytical solutions of these problems as true values. The maximum error was less than 2.4% for the relatively simple 2D Poiseuille and more complex 3D Womersley flow problems. The authors reported calculation verification being conducted with a focus on (1) discretization error, (2) numerical solver error, and (3) user error.

Validation: Sensitivity analysis was used to identify the input variables with the highest impact on the QoIs. Regarding the considered variables of density, viscosity, heart rate (HR), atrial pressure, ejection fraction (EF), and coefficients and resistances defining aortic and VAD flows, the sensitivity analysis identified the most relevant variables as HR, EF, and VAD coefficients.

The validation UQ analysis consisted of six validation experiments varying the previously mentioned variables. These validation experiments included ranges of HR, EF, as well as pump speed (to support answering the question of interest). The UQ results showed that better agreement was observed for mid-point working conditions, whereas the lowest level of agreement occurred when the pump operates at the high-speed condition, but the EF and HR values were in the considered range.

Table 3 LVAD implementation—risk map

Decision Consequence	Low	Med	High
High	3 ★	4	5
Med	2	3	4
Low	1	2	**3**

Model Influence

Applicability: Applicability assesses the relevance of the validation results to the COU. In this case, the COU focuses on the VAD and aortic flow to analyze the total cardiac output and aortic valve opening. The results indicated that the validation activities encompassed a subset of the validation points.

Summary: The model credibility assessment demonstrated that the model closely aligns with the validation points for the proposed simple COU. Although not all credibility factors achieved the highest possible score, they met or exceeded the target for medium-risk applications. For riskier applications, where the numerical model influences safety-related decisions, reaching a maximum score is crucial. The authors outline what further steps might be followed to further improve the model and achieve these optimal scores. Recognizing the rigorous application of VVUQ in this work, the authors extended the model to a ramp study to predict an operational speed range that allows aortic valve opening and desired total aortic flow.

8 Observations, Summary, and Future Directions

The transporting of blood and the design of blood pumps has progressed significantly from the initial work by Truax in 1899 using roller pumps. Recent advances in both computational modeling and experimental evaluation of blood pumps have greatly accelerated their development and capabilities. With its potential for providing longer-term circulatory support, we have focused this chapter on ventricular assist devices (VADs). Nevertheless, the material covered in this chapter can also be applied to other blood pumping technologies.

A ventricular assist device provides patients with circulatory support for periods ranging from several hours to several months to many years. Therefore, a high level of confidence in the VADs ability to support the patient is needed. This confidence is gained through a rigorous development and physical testing process. The development of VADs typically progresses from initial design work to in vitro hydraulic performance testing, to in vitro biocompatibility testing, to acute and then chronic in vivo animal testing, and finally to limited clinical trials. The evolution toward a final "preferred" design that is ready for clinical evaluation typically follows an iterative process that is guided by both CFD modeling and physical testing. CFD modeling is used to gain insight into the flow field throughout the VAD and help reduce the number of physical design iterations. The pump's clinical readiness is typically demonstrated through extensive and successful in vitro and in vivo studies using prototypes and then finished devices. If flow-related problems should arise through these studies, then CFD modeling is used to understand the potential root causes and propose design changes. The justification to proceed with clinical studies is currently based primarily upon the findings from in vitro and in vivo studies, supported as needed by CFD simulation results.

From the perspective of the ASME V&V 40 standard, numerous scenarios could be explored when considering the use of CFD modeling to help demonstrate the safety

and effectiveness of a VAD. Each scenario begins by defining a specific question of interest. Several potential questions of interest for VADs are:

- **Is the flow path design capable of achieving the hydraulic performance needed for ventricular support?**
- **Is the flow path design capable of achieving the biocompatibilityneeded for ventricular support?**
- **Can the VAD maintain ventricular support, considering both hydraulic performance and biocompatibility, under extreme operating or patient conditions?**

Physical testing would currently be used to validate the CFD modeling results and demonstrate pump performance for most of these scenarios, which would involve measuring hydraulic performance and/or blood damage-related quantities over a wide range of anticipated operating conditions. However, for the last scenario related to extreme conditions, it is possible that physical testing would not be attainable. Therefore, CFD results could provide the primary source of evidence supporting VAD safety.

A current snapshot of the many different blood pump-related performance parameters, their clinical significance, and validation methods is summarized in Table 4. Four levels of computational and experimental complexity are defined in the table in increasing order. Level 1 focuses on predicting hydraulic performance and device wash-out to demonstrate basic pump capabilities. In Level 2, regions of low and high shear stress are identified, which could correlate with increased thrombosis risk, cell lysis, or platelet activation. Level 3 incorporates additional equations in the CFD model to predict hemolysis or platelet activation. For example, Lagrangian methods that integrate the shear strain rate and exposure time along the particle pathlines, or Eulerian methods to calculate the hemolysis index (HI) or platelet activation level throughout the flow domain [40]. Then, in the highest Level 4, thrombus growth and a changing blood flow path, thrombus ingestion, and interaction of the VAD with the ventricle would be considered. Predicting the response of the blood to the flow conditions within the VAD is a common requirement for all performance parameters cited in the table. Building on the flow analysis, being able to reliably predict blood component activation and/or blood damage would enable full utilization and trust in the CFD simulation results.

The development of new CFD modeling methods for predicting the interaction of blood pumps and other cardiovascular devices with the blood and patient anatomy is accelerating. Organizations, such as the International Society for Mechanical Circulatory Support, Avicenna Alliance, and the Medical Device Innovation Consortium (MDIC) have programs focused on expanding the capabilities of computational modeling for medical devices. Their long-range goal is advancing the utilization of computational methods in regulatory submissions and as a standard of practice in the healthcare industry. Recently, a “digital twin” concept was introduced into the medical community which aims to create a virtual representation of a physical application [70]. In the context of this chapter, a digital twin of a patient and their implanted VAD would enable enhanced pump control through the exploration of different use

Table 4 Summary of pump performance parameters, clinical significance, and validation methods. Please see the references for details about each CFD modeling method and the corresponding validation activities

Level	Performance parameter	CFD modeling results	Clinical significance	Validation method(s)	References
1	Hydraulic performance	Predicted H-Q curves	Maintain cardiac output	In vitro measured H-Q curves (steady-state or transient conditions)	[54–56]
1	Device wash out	Passive scalar transport	Thrombosis risk	Residence time studies	[17, 54, 57]
				Dye or salt concentration studies	
2	Low blood shear stress	Shear stress or strain rate (contour/ histogram)	Thrombosis risk	Flow visualization (PIV)	[58–60]
				In vivo—animal testing (indirect/post implant method)	
2	High blood shear stress	Shear stress or strain rate (contour/ histogram)	Cell lysis or platelet activation	Flow visualization (PIV)	[61, 62]
				In vitro—hemolysis/ platelet activation testing	
				In vivo—animal testing	
3	Hemolysis index (HI)	Lagrangian or Eulerian HI	Red blood cell damage	In vitro—hemolysis testing	[40, 55, 63–65]
				In vivo—animal testing	
3	Platelet activation	Particle trajectories (shear stress and exposure time)	Thrombosis risk and platelet loss	In vitro testing	[46, 66, 67]
				In vivo—animal testing	
4	Thrombus formation	Thrombus modeling	Thrombosis risk and platelet loss	In vitro testing	[45, 47, 48, 68]
				In vivo—animal testing	
4	Thrombus ingestion	Discrete-phase particle models	Thrombosis risk	In vivo—animal testing	[69]
4	Ventricle interaction	Rigid CFD model with (a) steady-state or (b) transient flow conditions; fluid–structure (one-way or two-way) interaction models	Blood damage and thrombosis risk	In vitro experiments with anatomically representative flow paths	[51]
				EchoPIV	

cases and physiological conditions. This goal would require advancements in credibility assessment and regulatory frameworks, but is worthwhile when considering the long-term benefits to patients utilizing these therapies. We look forward to the realization of these ambitions and the further evolution of blood pumps and other devices to support the cardiovascular needs of all patients.

References

1. WHO. (2021). *Fact sheet*.
2. Goodwin, M. L., Lee, P. H. U., & Mokadam, N. A. (2020). Implantable continuous-flow blood pump technology and features. In *Mechanical support for heart failure* (pp. 337–358). Springer.
3. Boettcher, W., Merkle, F., & Weitkemper, H.-H. (2003). History of extracorporeal circulation: The invention and modification of blood pumps. *The Journal of The American Society of Extra-Corporeal Technology, 35*(3), 184–191.
4. Olsen, D. B. (2000). The history of continuous-flow blood pumps. *Artifical Organs, 24*(6), 401–404.
5. Mueller, J. P., Kuenzli, A., Reuthebuch, O., Dasse, K., Zuend, G., Turina, M. I., & Lachat, M. L. (2004). The CentriMag: A new aoptimized centrifugal blood pump with levitating impeller. *The Heart Surgery Forum, 7*(5), E477–E480.
6. Wampler, R. K., Moise, J. C., Frazier, O. H., & Olsen, D. B. (1988). In vivo evaluation of a peripheral vascular access axial flow blood pump. *Transactions of the American Society for Artificial Internal Organs, 34*, 450.
7. Tayama, E. Y., Ohashi, Y., Olsen, D. B., Benkowski, R., Morley, D., Noon, G. P., Nose, Y., & DeBakey, M. E. (1997). The Debakey Vad; Current status in 1997. *Artificial Organs, 21*(6), 518.
8. Macris, M., Myers, T., & Jarvik, R. (1994). In vivo evaluation of an intraventricular electric axial flow pump for left ventricular assistance. *ASAIO Journal, 40*, 719–722.
9. Singhvi, A., & Trachtenberg, B. (2019). Left ventricular assist devices 101: Shared care for general cardiologists and primary care. *Journal of Clinical Medicine, 8*(10), 1720–1744.
10. Motta, P. (2020). The congenital cardiac anesthesia society E-news. *Summer*. [Online]. Available: https://www2.ccasociety.org/newsletters/2020summer/HM3.html
11. Balachandran, I., Frazier, O. H., & Rogers, J. G. (2022). Doing the wrong thing for the right reasons: The demise of the HVAD. *The Journal of Thoracic and Cardiovascular Surgery, 164*, 1937–1941.
12. Kim, J. H., Cowger, J. A., & Shah, P. (2018). The evolution of mechanical circulatory support. *Cardiology Clinics, 39*, 443–449.
13. Akdis, M., & Reul, H. (2005). Mechanical blood pumps for cardiac assistance. *Applied Bionics and Biomechanics, 2*, 73–80.
14. Karimov, J. H., Fukamachi, K., & Starling, R. C. (2020). *Mechanical support for heart failure.* Springer.
15. Cheng, A., Williamitis, C. A., & Slaughter, M. S. (2014). Comparison of continuous-flow and pulsatile-flow left ventricular assist devices: Is there an advantage to pulsatility? *Annals of Cardiothoracic Surgery, 3*(6), 573–581.
16. Kumar, J., Elhassan, A., Dimitrova, G., & Essandoh, M. (2019). The lavare cycle: A novel pulsatile feature of the HVAD continuous-flow left ventricular assist device. *Journal of Cardiothoracic and Vacsular Anethesia, 33*(4), 1170–1171.
17. Boraschi, A., Bozzi, S., Thamsen, B., Granegger, M., Wiegmann, L., Pappalardo, F., Slepian, M., Kurtcuoglu, V., Redaelli, A., De Zelicourt, D., & Consolo, F. (2021). Thrombotic risk of rotor speed modulation regimes of contemporary centrifugal continuous-flow left ventricular assist devices. *ASAIO Journal, 67*(7), 737–745.

18. Wiegmann, L., Thamsen, B., Zelicourt, D., Granegger, M., Boes, S., Daners, M. S., Mebolt, M., & Kurtcuoglu, V. (2019). Fluid dynamics in the HeartMate 3: Influence of the artifical pulse feature and residual cardiac pulsation. *Artificial Organs, 43*(4), 363–376.
19. Mahmood, A. K., Courtney, J. M., Akdis, M., Reul, H., & Westaby, S. (2000). Critical review of current left ventricular assist devices. *Perfusion, 15*(5), 399–420.
20. Khelghatibana, M., Goodin, M. S., Yaksh, M., Horvath, D. J., Kuban, B. D., Fukamachi, K., & Karimov, J. H. (2022). Total artificial heart computational fluid dynamics: Modeling of stator bore design effects on journal-bearing performance. *ASAIO Journal, 68*(5), 655–662.
21. Kink, T., & Reul, H. (2004). Concept for a new hydrodynamic blood bearing for miniature blood pumps. *Artifical Organs, 28*(10), 916–920.
22. Kaya, D., Yagmur, E. A., Yigit, K. S., Kilic, F. C., Eren, A. S., & Celik, C. (2008). Energy efficiency in pumps. *Energy Conservation and Management, 49*(6), 1662–1673.
23. Khush, K. K., Cherikh, W. S., Chambers, D. C., Goldfarb, S., Kucheryavaya, A. Y., Levvey, B. J., Meiser, B., Rossano, J. W., & Stehlik, J. (2018). The international thoracic organ transplant registry of the international society for heart and lung transplantation: Thirty-fifth adult heart transplantation report—2018; Focus theme: Multiorgan transplantation. *The Journal of Heart and Lung Transplantation, 37*(10), 1155–1168.
24. Holman, W. A., & Kirklin, J. K. (2006). Outcomes after mechanical circulatory support. In *ISHLT monograph series: Mechanical circulatory support* (pp. 137–154). Elsevier.
25. Chan, C. H. H., Pieper, I. L., Hambly, R., Radley, G., Jones, A., Friedmann, Y., Hawkins, K. M., Westaby, S., Foster, G., & Thornton, C. A. (2015). The CentriMag centrifugal blood pump as a benchmak for in vitro testing of hemocompatibility in implantable ventricular assist devices. *Artificial Organs, 39*(2), 93–101.
26. Frazier, O. H. (2014). Mechanical circulatory assist device development at the Texas Heart Institute: A personal perspective. *The Journal of Thoracic and Cardiovascular Surgery, 147*(6), 1738–1744.
27. Roache, P. J. (1997). Quantification of uncertanity in computational fluid dynamics. *Annual Review of Fluid Mechanics, 29*, 123–160.
28. Wood, H., Anderson, J., Allaire, P., McDaniel, J., & Bearnson, G. (1999). Numerical solution for blood flow in a centrifugal ventricular assist device. *International Journal of Artificial Organs, 22*(12), 827–836.
29. Fraser, K. H., Taskin, M. E., Griffith, B. P., & Wu, Z. J. (2011). The use of computational fluid dynamics in the development of ventricular assist devices. *Medical Engineering & Physics, 33*(3), 263–280.
30. Thamsen, B., Blumel, B., Schaller, J., Paschereit, C. O., Affeld, K., Goubergrits, L., & Kertzscher, U. (2015). Numerical analysis of blood damage potential of the HeartMate II and HeartWare HVAD rotary blood pumps. *Artificial Organs, 39*(8), 651–659.
31. Cho, Y., & Kensey, K. (1991). Effects of the non-Newtonian viscosity of blood on flows in a diseased arterial vessel. Part 1: Steady flows. *Biorheology, 28*(3–4), 241–262.
32. Monreal, G., Koenig, S. C., Taskin, M. E., Shambaugh, C., LaRose, J. A., & Slaughter, M. S. (2023). Feasibility testing of the RT cardiac systems percutaneous mechanical circulatory support device. *ASAIO Journal, 69*(6), 519–526.
33. Menter, F. (1994). Two-equation eddy-viscosity turbulence models for engineering applications. *AIAA Journal, 32*(8), 1598–1605.
34. Menter, F. (2009). Review of the shear-stress transport turbulence model experience from an industrial perspective. *International Journal of Computational Fluid Dynamics, 23*(4), 305–316.
35. Mentor, F., & Lechner, R. (2021). Best practice: RANS turbulence modeling in Ansys CFD. [Online]. Available: https://www.ansys.com/content/dam/amp/2022/march/quick-request/Best%20Practice%20RANS%20Turbulence%20Modeling%20in%20Ansys%20CFD.pdf
36. Taskin, M. E., Fraser, K. H., Zhang, T., Gellman, B., Fleischli, A., Dasse, K. A., Griffith, B. P., & Wu, Z. J. (2010). Computational characterization of flow and hemolytic performance of the UltraMag blood pump for circulatory support. *Artificial Organs, 34*(12), 1099–1113.

37. Giersiepen, M., Wurzinger, L. J., Opitz, R., & Reul, H. (1990). Estimation of shear stress related blood damage in heart valve prostheses-in vitro comparison of 25 aortic valves. *International Journal of Artificial Organs, 13*, 300–306.
38. Heuser, G., & Opitz, R. (1980). A Couette viscometer for short time shearing of blood. *Biorheology, 17*, 17–24.
39. Zhang, T., Taskin, M. E., Fang, H. B., Pampori, A., Jarvik, R., Griffith, B. P., & Wu, Z. J. (2011). Study of flow-induced hemolysis using novel Couette-type blood-shearing devices. *Artificial Organs, 35*(12), 1180–1186.
40. Taskin, M. E., Fraser, K. H., Zhang, T., Wu, C., Griffith, B. P., & Wu, Z. J. (2012). Evaluation of eulerian and lagrangian models for hemolysis estimation. *ASAIO Journal, 58*(4), 363–372.
41. Farinas, M.-I., Garon, A., Lacasse, D., & N'dri, D. (2006). Asymptotically consistent numerical approximation of hemolysis. *Journal of Biomechanical Engineering, 128*(5), 688–696.
42. Goubergrits, L. (2006). Numerical modeling of blood damage: Current status, challenges and future prospects. *Expert Review of Medical Devices, 3*(5), 527–531.
43. Pirker, S., Schima, H., & Stoiber, M. (2005). Numerical simulation of hemolysis: A comparison of Lagrangian and Eulerian modelling. *WIT transactions on biomedicine and health, 8*, 361–370.
44. Faghih, M. M., Craven, B. A., & Sharp, M. K. (2023). Practical implications of the erroneous treatment of exposure time in the Eulerian hemolysis power law model. *Artificial Organs, 47*(9), 1531–1538.
45. Blum, C., Groß-Hardtb, S., Steinseifer, U., & Neidlin, M. (2022). An accelerated thrombosis model for computational fluid dynamics simulations in rotary blood pumps. *Cardiovascular Engineering and Technology, 13*(4), 638–649.
46. Marom, G., & Bluestein, D. (2016). Lagrangian methods for blood damage estimation in cardiovascular devices—How numerical implementation affects the results. *Expert Review of Medical Devices, 13*(2), 113–122.
47. Chiu, W., Slepian, M. J., & Bluestein, D. (2014). Thrombus formation patterns in the HeartMate II VAD-clinical observations can be predicted by numerical simulations. *ASAIO Journal, 60*(2), 237–240.
48. Taylor, J. O., Meyer, R. S., Deutsch, S., & Manning, K. B. (2016). Development of a computational model for macroscopic predictions of device-induced thrombosis. *Biomechanics and Modeling in Mechanobiology, 15*(6), 1713–1731.
49. (2018). *ASME V&V40 accessing credibility of computational modeling through verification and validation: Application to medical devices.* American Society of Mechanical Engineers.
50. Morrison, T. M., Hariharan, P., Funkhouser, C. M., Afshari, P., Goodin, M., & Horner, M. (2019). Assesing computational model credibility using a risk-based framework: Application to hemolysis in centrifugal blood pumps. *ASAIO Journal, 65*, 349–360.
51. Santiago, A., Butakoff, C., Eguzkitza, B., Gray, R. A., May-Newman, K., Pathmanathan, P., Vu, V., & Vazquez, M. (2022). Design and execution of a verification, validation, and uncertainty quantification plan for a numerical model of left ventricular flow after LVAD implantation. *Plos Computational Biology, 18*(6), 13.
52. Malinauskas, R. A., Hariharan, P., Day, S. W., Herbertson, L. H., Buesen, M., Steinseifer, U., Aycock, K. I., Good, B. C., Deutsch, S., Manning, K. B., & Craven, B. A. (2017). FDA benchmark medical device flow models for CFD validation. *ASAIO Journal, 63*(2), 150–160.
53. Hariharan, P., Aycock, K. I., Buesen, M., Day, S. W., Good, B. C., Herbertson, L. H., Steinseifer, U., Manning, K. B., Craven, B. A., & Malinauskas, R. A. (2018). Inter-laboratory characterization of the velocity field in the FDA blood pump model using particle image velocimetry (PIV). *Cardiovascular Engineering and Technology, 9*(4), 623–640.
54. Goodin, M. S., Showalter, M. S., Horvath, D. J., Kuban, B. D., Flick, C. R., Polakowski, A. R., Fukamachi, K., & Karimov, J. H. (2022). Characterization and development of universal ventricular assist device: Computational fluid dynamics analysis of advanced design. *ASAIO Journal, 68*(8), 1024–1035.
55. Zhang, J., Gellman, B., Koert, A., Dasse, K. A., Gilbert, R. J., Griffith, B. P., & Wu, Z. J. (2006). Computational and experimental evaluation of the fluid dynamics and hemocompatibility of the CentriMag blood pump. *Artificial Organs, 30*(3), 168–177.

56. Burgreen, G. W., Loree, H. M., II., Bourque, K., Dague, C., Poirier, V. L., Farrar, D., Hampton, E., Wu, Z. J., Gempp, T. M., & Schob, R. (2004). Computational fluid dynamics analysis of a maglev. *Artificial Organs, 28*(10), 874–880.
57. Molteni, A., Masri, Z. P., Low, K. W., Yousef, H. N., Sienz, J., & Fraser, K. H. (2018). Experimental measurement and numerical modeling of dye washout for investigation of blood residence time in ventricular assist devices. *International Journal of Artificial Organs, 41*(4), 201–212.
58. Hochareon, P., Manning, K. B., Fontaine, A. A., Tarbell, J. M., & Deutsch, S. (2004). Correlation of in vivo clot deposition with the flow characteristics in the 50 cc Penn State artificial heart: A preliminary study. *ASAIO Journal, 50*(6), 537–542.
59. Mendez Rojano, R., Lai, A., Zhussupbekov, M., Burgreen, G. W., Cook, K., & Antaki, J. F. (2022). A fibrin enhanced thrombosis model for medical devices operating at low shear regimes or large surface areas. *PLoS Computational Biology, 18*(10), 1–22.
60. Goodin, M. S., Horvath, D. J., Kuban, B. D., Polakowski, A. R., Fukamachi, K., Flick, C. R., & Karimov, J. H. (2022). Computational fluid dynamics model of continuous-flow total artificial heart: Right pump impeller design changes to improve biocompatibility. *ASAIO Journal, 68*(6), 829–838.
61. Good, B., & Manning, K. (2020). Computational modeling of the Food and Drug Adminstration's benchmark centrifugal blood pump. *Artifical Organs, 44*(7), 263–276.
62. Hellums, J. D., Peterson, D. M., Stathopoulos, N. A., Moake, J. L., & Giorgio, T. D. (1987). Studies on the mechanisms of shear-induced platelet activation. In *Cerebral ischemia and hemorheology*, pp. 80–89. Springer.
63. Garon, A., & Farinas, M. I. (2004). Fast three-dimensional numerical hemolysis approximation. *Artificial Organs, 28*(11), 1016–1025.
64. Wu, P., GroB-Hardt, S., Boehning, F., & Hsu, P. (2020). An energy-dissipation-based power-law formulation for estimating hemolysis. *Biomechanics and Modeling in Mechanobiology, 19*(2), 591–602.
65. Arora, D., Behr, M., & Pasquali, M. (2004). A tensor-based measure for estimating blood damage. *Artificial Organs, 28*(11), 1002–1015.
66. Ding, J., Chen, Z., Niu, S., Zhang, J., Mondal, N. K., Griffith, B. P., & Wu, Z. J. (2015). Quantification of shear-induced platelet activation: High shear stresses for short exposure time. *Artificial Organs, 39*(7), 576–583.
67. Slepian, M. J., Alemu, Y., Silva Soares, J., Smith, R. G., Einav, S., & Bluestein, D. (2013). The syncardia total artificial heart: In vivo, in vitro, and computational modeling studies. *Joural of Biomechanics, 46*(2), 266–275.
68. Wu, W. T., Jamiolkowski, M. A., Wagner, W. R., Aubry, N., Massoudi, M., & Antaki, J. F. (2017). Multi-constituent simulation of thrombus deposition. *Scientific Reports, 7*(42720).
69. Rowlands, G., Pagani, F. D., & Antaki, J. (2020). Classification of the frequency, severity, and propagation of thrombi in the HeartMate II left ventricular assist device. *ASAIO Journal, 66*(9), 992–999.
70. Horner, M. (2019). *Multi-physics, multi-scale, system-level modeling.* Ansys Software. [Online]. Available: https://www.imagwiki.nibib.nih.gov/sites/default/files/Horner_ANSYS_IMAGMSMSeminar_DigitalTwin_20191004.pdf

Advance medical-device development with credible simulation

From early design exploration through verification, validation, and regulatory support, credible computational modeling can help medical-device teams evaluate performance, reduce development risk, and make better-informed engineering decisions.

SimuTech Group supports medical-device organizations with advanced simulation software, engineering consulting, training, technical support, and model-development expertise across applications including:

- Blood-flow and cardiovascular-device modeling
- Fluid-structure interaction
- Hemolysis and thrombosis assessment
- Verification, validation, and uncertainty quantification
- Thermal, structural, and electromagnetic simulation
- Simulation workflows for design and regulatory decision-making

Our engineers work alongside internal product-development, research, and regulatory teams to develop practical, defensible simulation approaches grounded in sound engineering methods.

Talk with a SimuTech expert

Explore how simulation can support your next medical-device project.

Visit simutechgroup.com or Contact SimuTech Group